NEUTRINO FACTORY/MUON COLLIDER FRONT END SIMULATION COMPARISONS AND ECONOMIZATION OF RF CAVITIES *

C. Yoshikawa[†], Muons, Inc., Batavia IL, USA
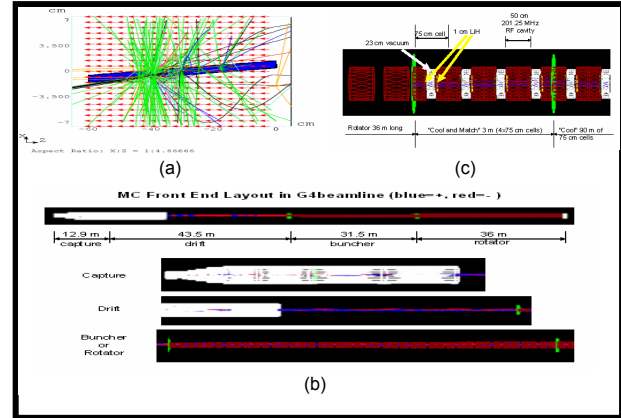D. Neuffer, Fermilab, Batavia, IL, USA

Figure 1: Layout of front end of a neutrino factory or muon collider. (a) Protons (black line) of 8 GeV (kinetic energy) and 3 ns rms impinge on Hg target with MARS-like [5] geometry. (b) The capture, drift, buncher, and rotator portions. (c) The "Cool and Match" and "Cool" sections where "cool and match" refer to magnetic fields that transition from solenoidal field in rotator to alternating solenoids in cooler.

Abstract

Earlier studies on the front end of a neutrino factory or muon collider have relied on a single simulation tool, ICOOL. We present here a cross-check against another simulation tool, G4beamline. We also perform a study in economizing the number of RF cavity frequencies and gradients. We conclude with a discussion of future studies.

INTRODUCTION

One of the major challenges in realizing a neutrino factory or muon collider is establishing a front end that captures and cools a sufficiently large number of muons that feed the downstream accelerating structures. The current baseline study 2A [1] for a neutrino factory or muon collider relied on ICOOL [2] for much of its design. A cross check is presented here utilizing G4beamline (G4BL) [3], which is based on GEANT4 [4]. Beyond the consistency verification, a preliminary study is performed on economizing the number of RF cavity frequencies and gradients. We conclude with a discussion of future studies.

CONSISTENCY VERIFICATION BETWEEN ICOOL AND G4BEAMLINE

The layout of the front end that is studied is a snapshot of an evolving design based on Study 2A [1] and is shown in Figure 1, along with some parameters listed in Table 1. The ICOOL and G4 beamline simulations used the same input events generated by MARS [5] simulations of a MERIT-like target system [6], in which protons of 8 GeV (kinetic energy) impinge on a jet stream of mercury. Both the protons and the Hg jet are at angles relative to the nominal z-axis that defines the geometry of the front end.

Snapshots in momentum vs. time for the evolution of pions and muons from start of the capture (tapered) solenoid to end of cooler are shown in Figure 2. Qualitatively, there is agreement between ICOOL and G4beamline, except at the end of the channel where muons in G4beamline have higher average momenta and a wider momentum spread compared to its ICOOL counterpart. We consider the following possible sources to account for theses differences:

1. Different rates of energy loss (dE/dx) for muons traversing LiH between ICOOL vs. G4beamline in "Cool and Match" and "Cool" sections. The remedy is to adjust the value of RF phase according to different energy loss.
2. A different algorithm for RF phasing in ICOOL and G4beamline that may be more pronounced in volumes with material.

Table 1: Parameters of the neutrino factory or muon collider front end layout.

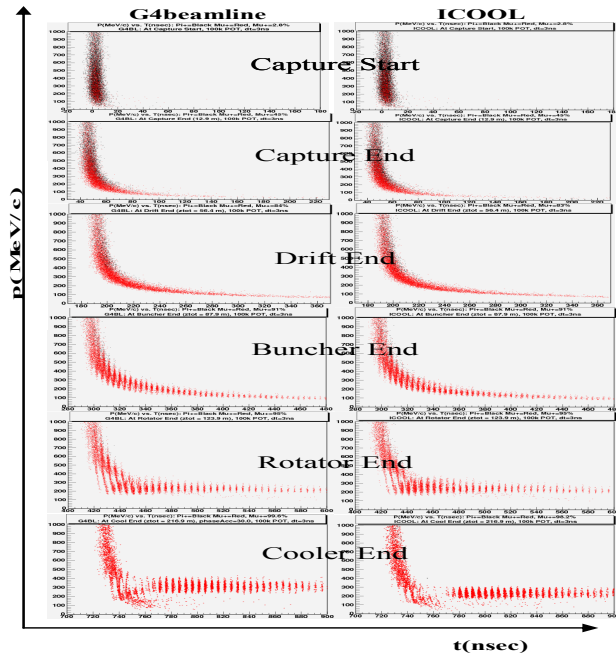| z(m)	Subsystem	Purpose	Physical Dimensions	Fields
−0.60 to 0.0	Targetry (MARS)	Produce copious pions	L ≈ 0.60 m R = 0.075 m	Bsol = 20 T
0.0 to 12.9	Capture/ Tapered Solenoid	Enhance pion/muon capture	L = 12.9 m R = 0.075 m →0.30 m	Bsol = 20 T → 2 T
12.9 to 56.4	Drift	Develop p/t correlation	L = 43.5 m R = 0.30 m	Bsol = 2 T
56.4 to 87.9	Buncher	Adiabatically capture muons into RF buckets	L = 31.5 m R = 0.30 m	Bsol = 2 T 42 RF Cavities: Ez,max = 0 →15 MV/m f = 367 MHz →238 MHz
87.9 to 123.9	Rotator	Energy-phase rotation	L = 36 m R = 0.30 m	Bsol = 2 T 48 RF cavities Ez,max = 15 MV/m f = 238 MHz →202 MHz
123.9 to 126.9	Cool and Match	Transition from B=2T in rotator to alternating solenoidal B in cooler.	L = 3 m R = 0.30 m	Bsol = 2 T → 2.3 T → −2.8 T 4 RF cavities Ez,max = 16 MV/m f=201.25 MHz
126.9 to 216.9	Cool	Cool muon beam	L = 90 m R = 0.30 m	Bsol = −2.8 T ↔ +2.8 T 120 RF cavities Ez,max = 16 MV/m f=201.25 MHz

Figure 2: Momentum (MeV/c) vs. time (nsec) from start of capture solenoid (exit of production via MARS) to end of cooler for G4beamline (left plots) and ICOOL (right plots) for μ^+s (red) and π^+s (black). Negative μ^-s and π^-s exhibit similar behavior.

To study the differences between ICOOL and G4beamline in their characterization of the cooling material (LiH), μ^+s were tracked through the cooling channel, without RF or magnetic fields for both simulators. The energy profile of the average muon energy is shown Figure 3.
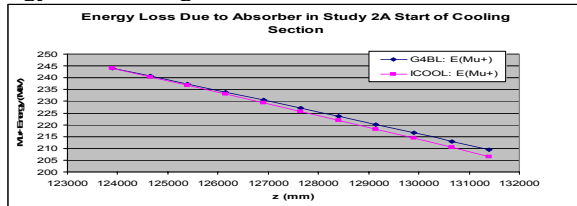

Figure 3: Energy loss in LiH for ICOOL and G4beamline. Packing factor of LiH is 2cm/75cm = 0.02667. Resultant losses are $dE/dx\big|_{ICOOL} \approx 1.87$ MeV/cm and $dE/dx\big|_{G4BL} \approx 1.73$ MeV/cm, an approximately 8% difference.

The energy loss rate in G4BL relative to ICOOL is about 8% less. If one were to scale this difference, the 30° RF phase in ICOOL would correspond to 27.4° in G4beamline. However, instead of extrapolating the result (based on 7.5 m) over the lengthy 93 m channel, we performed an optimal phase determination in G4beamline by propagating muons from the start of the cooling channel with p=220 MeV/c and maintaining that momentum across the channel; the optimal phase extracted in this way is 25.8° and is used below.

Next, we investigate the effects of the different methods of RF phasing with respect to the reference particle. ICOOL sets the phasing of RF cavities with respect to a reference particle at constant velocity, ignoring slow down across material and speed up in RF cavities.

G4beamline sets its phasing of RF cavities with respect to a reference particle, which does take into account the expected slow down in material and speed up in RF cavities. A direct comparison was performed within G4beamline to model both types of phasing in order to eliminate complications from other differences between ICOOL and G4beamline. The results in Figure 4 show effectively no effect due to the different phasing algorithms.
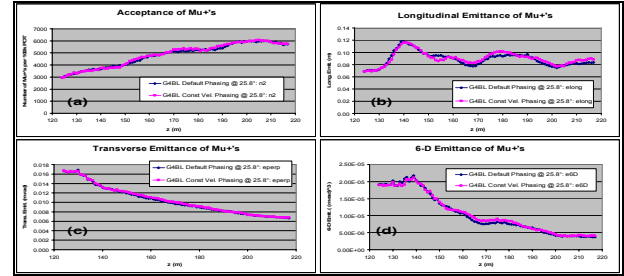

Figure 4: Effect of the ICOOL phasing method (constant velocity) vs. G4beamline phasing method (deceleration in material; acceleration in RF). Quantities are calculated using ECALC9. (a) Acceptance with cuts $A_{trans} < 0.030$ m-rad, $A_{long} < 0.15$ m-rad, and $n_\sigma < 6.0$. (b) Longitudinal Emittance. (c) Transverse Emittance. (d) 6-D Emittance.

Finally, we show in Figure 5 the acceptance and emittance through the front end expected from both G4beamline (phase 25.8°) and ICOOL (phase 30.0°). There is a ~16% difference in the acceptance at the end of the cooling channel that is not currently understood, but is probably related to the larger amount of cooling provided in ICOOL (larger dE/dx in LiH and larger RF phase angle). This is currently under investigation as well as differences in multiple scattering models.
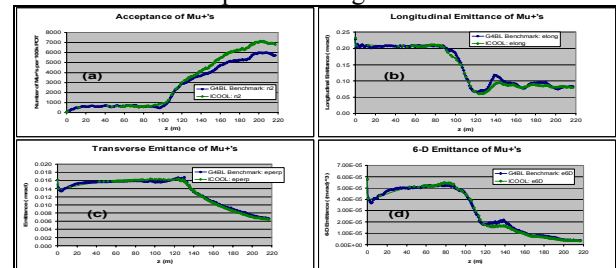

Figure 5: ICOOL vs. Benchmark G4beamline (G4BL) across front end. Benchmarked G4BL uses phase of 25.8° to account for differences in dE/dx in LiH. Quantities are calculated using ECALC9. (a) Acceptance with cuts $A_{trans} < 0.030$ m-rad, $A_{long} < 0.15$ m-rad, and $n_\sigma < 6.0$. (b) Longitudinal Emittance. (c) Transverse Emittance. (d) 6-D Emittance.

Figure 6 shows internal consistency when the same equilibrium cooling momentum (220 MeV/c) is targeted in both G4beamline and ICOOL, obtaining similar momentum vs. time distributions for muons (and pions) at the end of the cooling channel using a phase of 25.8° in G4beamline and 30° in ICOOL. This is to be compared to the last pair of plots in Figure 2, which utilized 30.0° for both simulators.
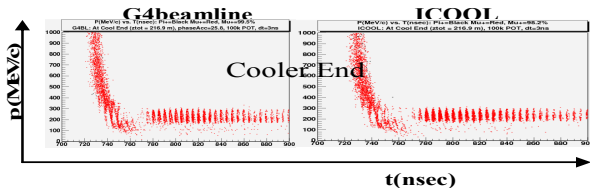
Figure 6: Momentum (MeV/c) vs. time (nsec) at end of cool section using phase of 25.8° in G4beamline (G4BL) and 30.0° for ICOOL.

ECONOMIZATION OF RF CAVITIES

A study was done to understand the sensitivity of the buncher and rotator sections with respect to the granularity of frequencies and gradients used. The investigation was performed entirely in G4beamline, so complications from differences between G4BL and ICOOL are avoided. The benchmark study allowed each RF cavity to implement its own ideal frequency based on two reference particles of different momenta being separated by a pre-selected number of RF wavelengths. In this particular case, we used 280 MeV/c and 154 MeV/c separated by 10 wavelengths in the buncher and 10.08 wavelengths in the rotator. Additionally, each RF cavity in the buncher had its maximum gradient rise according to:

$$G(MV/m) = (6MV/m)(z/31m) + (9MV/m)(z/31m)^2 \quad (1)$$

where z is the longitudinal location within the buncher. The maximum gradient in the rotator is 15 MV/m.

To test the sensitivity of the algorithm against the granularity of frequencies and field gradients, we grouped the cavities as follows:

1. Cavities in buncher and rotator were grouped into threes, where the set used a common frequency and gradient set by the middle cavity (Grp3RF)
2. Cavities in buncher and rotator were grouped into sixes, where the set used a common frequency and gradient set by average of the middle two cavities (Grp6RF)
3. Cavities in the buncher grouped into threes and cavities in the rotator grouped into sixes (Grp3&6RF) with frequencies and gradients set as in (1) and (2) above.
4. Cavities in the buncher grouped into sixes and cavities in the rotator grouped into threes (Grp6&3RF) with frequencies and gradients set as in (1) and (2) above.

Results for the acceptance and longitudinal emittance are shown in Figure 7, while transverse and 6-D emittances are in Figure 8. Differences in acceptance and emittances in the buncher and rotator sections appear minimal until they are propagated through the cooling channel where the differences in acceptance are magnified. We could realize cost savings associated with RF cavities using a common frequency and gradient in groups of three with only an expected ~5% reduction in acceptance at 200 m.
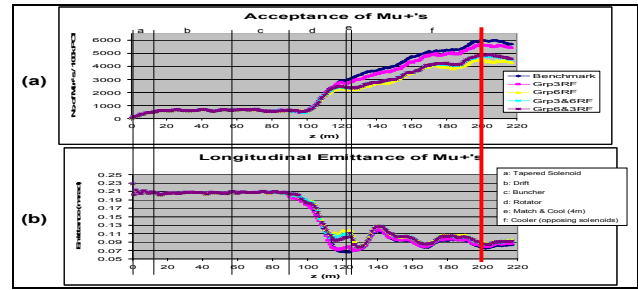

Figure 7: Economization of RF frequencies and gradients in buncher and rotator. Quantities are calculated using ECALC9. (a) Acceptance with cuts $A_{trans} < 0.030$ m-rad, $A_{long} < 0.15$ m-rad, and $n_\sigma < 6.0$. (b) Longitudinal emittance.
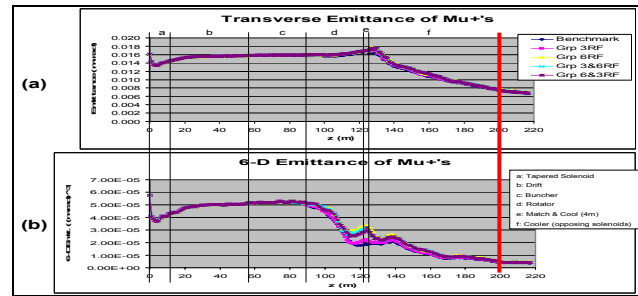

Figure 8: Economization of RF frequencies and gradients in buncher and rotator. Quantities are calculated using ECALC9. (a) Transverse emittance. (b) 6-D emittance.

CONCLUSION

We observe consistency between ICOOL and G4beamline in modeling the baseline design for the front end of a neutrino factory/muon collider, except in the cooling section, where the disparities are due to a difference in the modeling of the LiH cooling material. We will need to verify this and determine which simulator is more accurate.

Within G4beamline, we studied the different RF phasing algorithms and saw no effective differences between ICOOL's constant velocity phasing and G4beamline's reference tracking based phasing that takes into account slow down in material and speed up in RF cavities.

A preliminary study to economize the number of RF frequencies and gradients, also having relevance to tolerances expected of the system, showed that we can reduce the number of frequencies and gradients by a factor of three at a price of reducing acceptance by about 5%.

REFERENCES

[1] "Cost-effective Design for a Neutrino Factory", J. S. Berg *et al.*, **Phys. Rev. STAB 9**, 011001(2006)
[2] ICOOL: R. Fernow, http://pubweb.bnl.gov/users/fernow/www/icool/
[3] G4beamline: T. Roberts, http://g4beamline.muonsinc.com
[4] GEANT4: http://www.geant4.org/geant4/
[5] MARS: N. Mokhov, http://www-ap.fnal.gov/MARS/
[6] MERIT: http://cern.ch/merit/